Brain and Spine 2 (2022) 100856

Contents lists available at ScienceDirect

Brain and Spine

journal homepage: www.journals.elsevier.com/brain-and-spine

Sensitivity of three-dimensional time-of-flight 3.0 T magnetic resonance angiography in visualizing the number and course of lenticulostriate arteries in patients with insular gliomas

Andrey E. Bykanov [a], David I. Pitskhelauri [a], Artem I. Batalov [b], Robert Young [c,d], Maxim A. Trube [f,*], Andrei I. Holodny [c,d,e], Igor N. Pronin [b], Timur Zagidullin [a]

[a] Department of Neuro-oncology, Moscow, Russia
[b] Neuroradiology (A.I.B., I.N.P.) N.N, Burdenko National Medical Research Center of Neurosurgery of the Ministry of Health of the Russian Federation, Moscow, Russia
[c] Department of Radiology, Memorial Sloan Kettering Cancer Center, New York, NY, USA
[d] Department of Radiology, Weill Medical College of Cornell University, 525 East 68th Street, New York, NY, 10065, USA
[e] Department of Neuroscience, Weill-Cornell Graduate School of the Medical Sciences, 1300 York Ave, New York, NY, 10065, USA
[f] Peoples' Friendship University of Russia, Faculty of Medicine, Moscow, Russia

ARTICLE INFO

Keywords:
Lenticulostriate arteries
Insular glioma
3D TOF
Time-of -flight MRA
Neuro-oncology

ABSTRACT

Background: Neurosurgical resection of insular gliomas is complicated by the possibility of iatrogenic injury to the lenticulostriate arteries (LSAs) and is associated with devastating neurological complications, hence the need to accurately assess the number of LSAs and their relationship to the tumor preoperatively.
Methods: The study included 24 patients with insular gliomas who underwent preoperative 3D-TOF MRA to visualize LSAs. The agreement of preoperative magnetic resonance imaging with intraoperative data in terms of the number of LSAs and their invasion by the tumor was assessed using the Kendall rank correlation coefficient and Cohen's Kappa with linear weighting. Agreement between experts performing image analysis was estimated using Cohen's Kappa with linear weighting.
Results: The number of LSAs arising from the M1 segment varied from 0 to 9 (mean 4.3 ± 0.37) as determined by 3D-TOF MRA and 2–6 (mean 4.25 ± 0.25) as determined intraoperatively, $\kappa = 0.51$ (95% CI: 0.25–0.76) and $\tau = 0.64$ ($p < 0.001$). LSAs were encased by the tumor in 11 patients (confirmed intraoperatively in 9 patients). LSAs were displaced medially in 8 patients (confirmed intraoperatively in 8 patients). The tumor partially involved the LSAs and displaced them in 5 patients (confirmed intraoperatively in 7 patients), $\kappa = 0.87$ (95% CI: 0.70–1), $\tau = 0.93$ ($p < 0.001$). 3D-TOF MRA demonstrated high sensitivity (100%, 95% CI: 0.63–1) and high specificity (86.67%, 95% CI: 0.58–0.98) in determining the LSA–tumor interface.
Conclusions: 3D-TOF MRA at 3T demonstrated sensitivity in determining the LSA–tumor interface and the number of LSAs in patients with insular gliomas.

1. Introduction

Glial tumors account for up to 40–50% of all primary brain tumors, and a significant proportion of these tumors (25% of all low-grade and 10% of all high-grade gliomas) arise from or involve the insula (Duffau and Capelle, 2004). The first stage in the treatment of intrinsic insular tumors according to modern standards is their microsurgical removal (Weller et al., 2017). Despite advances in neurosurgery, the resection of intrinsic insular tumors remains a daunting task (Hervey-Jumper and Berger, 2019), leading to a high incidence of postoperative neurological deficits primarily related to the complex surgical anatomy of this area. The cortex of the insula is covered by the frontal, temporal, and parietal opercula and does not extend to the superficial surface of the brain. Medial to the insular lobe are the basal ganglia, internal capsule, which are supplied by the lenticulostriate arteries (LSAs).

LSAs are small-diameter (0.3–1.2 mm) branches of the M1 segment of the middle cerebral artery. Although the number of LSAs varies from 1 to 21 Bykanov et al., 2015; Marinković et al., 2001; Türe et al., 2000; Umansky, 1985, the occlusion of even one artery can lead to an extensive infarction of the subcortical ganglia and the internal capsule because

* Corresponding author.
E-mail address: maximtrube0@gmail.com (M.A. Trube).

https://doi.org/10.1016/j.bas.2021.100856
Received 8 October 2021; Received in revised form 17 December 2021; Accepted 19 December 2021
Available online 21 December 2021

there is no collateral blood supply between the LSAs Marinković et al., 2001. Injury to any individual LSA during insular surgery can cause severe and irreversible neurological deficits, including persistent hemiparesis due to ischemic damage to the internal capsule) (Eseonu et al., 2017; Hameed et al., 2019; Hentschel and Lang, 2005; Lang et al., 2001; Wang et al., 2017. As a result, the preoperative detection of the intraparenchymal courses and the location of LSAs relative to the tumor margins is of particular importance as a factor in the selection and planning of patients for surgical treatment. In cases where glial tumors involve the LSAs, the feasibility of radical tumor removal without neurological deficit is significantly reduced (Kawaguchi et al., 2014; Moshel et al., 2008). Tumor involvement of LSAs significantly increases the likelihood of persistent neurological deficit and decreases the overall survival rate (Kawaguchi et al., 2014; Moshel et al., 2008).

A non-invasive method of preoperative visualization of LSAs that is widely used in clinical practice is three-dimensional time-of-flight magnetic resonance angiography (3D-TOF MRA) (Bykanov et al., 2015; Rao et al., 2018; Saito et al., 2009) (Table 2). However, the specificity and sensitivity of this method in determining the number and course of perforating arteries of such a small diameter remain unknown. The goal of the present study is to evaluate whether 3D-TOF MRA can successfully determine the number of LSAs and their relation to tumor tissue in patients with insular gliomas of the brain compared to intra-operative evaluation.

2. Materials and methods

The present, prospective study was approved by The Ethics Board of our institution in accordance with the 1964 Helsinki Declaration and its later amendments. Written informed consent was obtained from each patient who participated in this study.

2.1. Patient selection

During the period from June 2012 to March 2018, 59 preoperative 3D-TOF MRA studies were performed at our institute to determine the course, relation to tumor margins, and number of LSAs in patients with presumed glial insular lobe tumors. The inclusion criteria for the study were: 1) pathologically proven glial tumor in the insula; 2) absence of contraindications to MRI; 3) microsurgical removal of the tumor as the first stage of treatment; 4) adequate intraoperative evaluation of the number of LSAs and their relation to tumor. Metastases and nonglial tumors were excluded from the study, because they were not likely to be infiltrative and encase the LSAs. 24 patients met the inclusion criteria and were included in the study.

2.1.1. Preoperative imaging protocol

Magnetic resonance imaging (MRI) was performed (Signa HDxt 3.0 T, GE Healthcare, Milwaukee, WI, USA) according to the following protocol: T2 (slice thickness = 3 mm), T2 CUBE (slice thickness = 0.8 mm), FLAIR-CUBE (slice thickness = 0.8 mm), diffusion-weighted imaging and FSPGR (slice thickness = 1 mm) sequences before intravenous contrast and FSPGR (slice thickness - 1 mm). All patients underwent 3D-TOF MRA without contrast enhancement. 3D-TOF MRA was performed in the axial plane using a gradient echo pulse sequence with the following parameters: repetition time (TR) = 19 ms, echo time (TE) = 3.4 ms, flip angle = 18°, field of view = 240 mm, matrix = 1024 × 1024, slice thickness = 1.2 mm, gap between the slices in the reconstruction = 0.3 mm, and voxel size = 0.234 × 0.234 × 1.2 mm. The 3D-TOF MRA images were used to create maximum intensity projections on an ADW (GE Healthcare, Milwaukee, WI, USA) workstation. The total time of the MRI study was 40–45 min. LSAs were identified as linear hyperintense signals arising from the M1 segment of the middle cerebral artery and continuing into the subcortical nuclei and the internal capsule.

2.1.2. Image post-processing and analysis

For more accurate visualization of tumor tissue margins, a combination of coronal T2 images and MR angiography was displayed on the Advantage Windows (AW) server 3.2 Ext 2.0 workstation using the SynchroView and NeuroRegistration software (GE Healthcare, Milwaukee, WI, USA). Image analysis (number, course, and relation of LSAs to tumor tissue) was performed independently by two neuroradiologists with more than 5 years of experience each, and in cases of discrepancy between the results, the opinion of a third expert (neuroradiologist, with more than 15 years of experience) was used to reach consensus. Encasement of the LSA was defined using 3D TOF MRA fused with 3DT2 CUBE/3DT2FLAIR-CUBE images.

Three variants (Fig. 1) of the relationship between the tumor and LSA were identified: I - all LSAs were completely encased by the tumor; II - LSAs were partially encased by the tumor; and III - LSAs displaced medially without signs of tumor growth around arteries. The tumor volume was measured in every patient before and after surgery.

Segmentation and volume measurements were performed pre- and postoperatively in the axial plane on AW workstation (AW Volume Share 5, GE,USA). The tumor volume was estimated on T2 and FLAIR images.

2.1.3. Surgical approach

In all patients, the trans-sylvian approach was used to access the insular lobe. In two patients this approach was supplemented with an opercular resection. Proximal dissection of the sylvian fissure was performed until the insula was reached, the M1 segment of the middle cerebral artery was exposed, and when it became possible to visualize the LSAs. Intraoperative indocyanine green fluorescence angiography was used to optimize LSA identification and counting.

Evoked motor potential monitoring (Nicolet Viking Select device; Natus) was conducted in all cases. Two methods for brain stimulation were used: transcranial and direct cortical stimulation. Neuro-navigation system (Medtronic, StealthStation S7) with tractography and intraoperative ultrasound (BK Medical, Pro Focus) were used to aid tumor excision.

Post-operative deficits were defined as the development of a new neurological deficit, or the deterioration of the existing deficit of motor function in the immediate post-operative period. If the neurological deficit persisted for three months postoperatively, it was considered as permanent.

2.1.4. Statistical analysis

Statistical software R v3.6.0 (IBM, Armonk, NY, USA) was utilized for statistical analysis. Continuous variables were presented as means and standard deviations. Cohen's kappa with linear weighting was used to test interrater reliability. The number of LSAs determined by 3D-TOF MRA was assessed against intraoperative data using the Kendall rank correlation coefficient and Cohen's kappa. The sensitivity and specificity of each method to determine the number of arteries were calculated. Odds ratio with 95% CI was calculated for a new motor neurological deficit in the early postoperative period (<24 h after surgery) for patients with variant II or III (LSAs displaced medially or partially encased by the tumor) versus patients with variant I (LSAs completely encased by the tumor) of the LSA–tumor interface.

3. Results

The study included 11 male and 13 female patients. Patient age ranged from 21 to 60 years (median, 35.2). In 11 (46%) patients, the tumor was in the left hemisphere; in the remaining 13 (54%) patients, the tumor was in the right hemisphere. According to the 2016 World Health Organization (WHO) classification, tumors were: diffuse astrocytoma, isocitrate dehydrogenase (IDH)-mutant (n = 14, 58.3%; WHO grade II); diffuse astrocytoma, IDH-wildtype (n = 1, 4.1%; WHO grade II); oligodendroglioma, IDH-mutant and 1p/19q-codelected (n = 3, 12.5%; WHO grade II); anaplastic astrocytoma, IDH mutant (n = 4, 16.7%; WHO grade

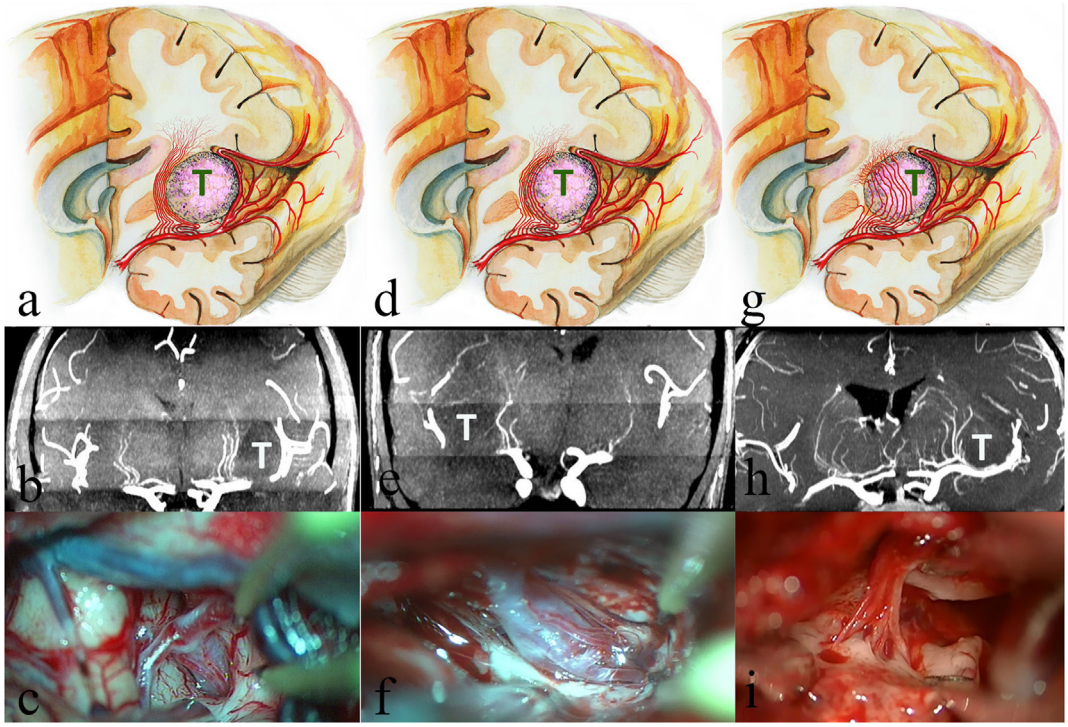

Fig. 1. Three variants of the LSA–tumor interface.
a, b, c: variant III: LSAs are displaced medially by the glioma of the left insular lobe (T), without signs of tumor growth around arteries. Anatomical drawing (a), coronal 3D-TOF MRA image (b), and intraoperative photo of the same patient (c).
d, e, f: variant II: partial tumor invasion of the arteries with medial displacement of the LSAs. Anatomical drawing (d), coronal 3D-TOF MRA image (e), and intraoperative photo of the same patient (f).
g, h, i: variant I: LSAs are encased by the tumor. Anatomical drawing (g), coronal 3D-TOF MRA image (h), and intraoperative photo of the same patient (i).

III); and anaplastic oligodendroglioma IDH-mutant and 1p/19q-codelected (n = 2, 8.3%; WHO grade III).

The median tumor volume before surgery was 56.6 cm^3. The median residual tumor volume after surgery was 4.72 cm^3.

Using 3D-TOF MRA, agreement between experts was high for determining the number of LSAs ($\kappa = 0.90$ [95% CI: 0.80–1]) as well as for determining the LSA–tumor interface ($\kappa = 1$) [95% CI: 1; 1]. Using 3D-TOF MRA, the number of LSAs arising from the M1 segment of the middle cerebral artery was determined to range from 0 to 9 (mean 4.3 ± 0.37). Intraoperatively, the number of lenticulostriate arteries arising from the M1 segment of the middle cerebral artery was determined to range from 2 to 6 (mean 4.25 ± 0.25). 3D-TOF MRA and intraoperative methods were significantly correlated: $\kappa = 0.51$ (95% CI: 0.25–0.76) and $\tau = 0.65$ ($p < 0.001$).

Three variants (Figs. 1 and 2) of the LSA–tumor interface were identified (Table 1). When comparing 3D-TOF MRA with intraoperative visualization in terms of encasement by tumor tissue, 3D-TOF MRA was significantly correlated with intraoperative visualization: $\kappa = 0.87$ (95% CI: 0.70–1); $\tau = 0.93$ ($p < 0.001$). 3D-TOF MRA also demonstrated high sensitivity (100%, 95% CI: 0.63–1) and high specificity (86.67%, 95% CI: 0.58–0.98) in determining the LSA–tumor interface.

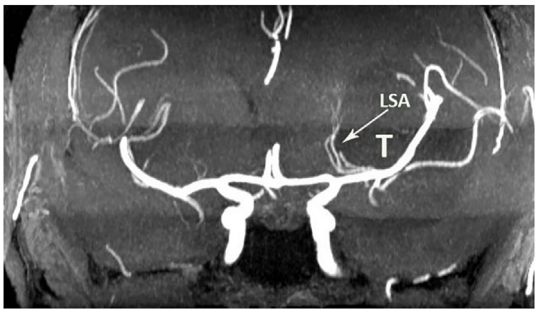

Fig. 2. Variant III of the LSA–tumor interface. LSAs (arrow) are displaced by tumor tissue in the medial direction and form an arcuate bend along the medial margin of the tumor.

3.1. Surgical outcomes

In the early postoperative period (24 h after surgery), a new motor neurological deficit related to LSA injury was observed in 6 (25%) patients (3 patients with variant I of the LSA–tumor interface, 2 patients with variant II, 1 patient with variant III). The odds ratio (variant II or III vs variant I) was 3.18 (95% CI: 0.30–33.26) but was not statistically significant. In one patient (4%), direct damage of the internal capsule without signs of ischemia on DWI was recorded. In this patient, the patient's paresis was due to iatrogenic injury to the internal capsule and not to injury of the LSAs. Three months after surgery, permanent neurological deficit was observed in only 1 (4.1%) patient (variant I of the LSA–tumor interface).

4. Discussion

The visualization of LSAs has clinical importance in both neurology and neurosurgery. In neurology, many articles have demonstrated a statistically significant correlation between the number of LSAs and the risk of developing hypertension (Chen et al., 2011, 2016), cerebral perforating artery disease, and deep cerebral infarction (Kang et al., 2010; Liang et al., 2019; Seo et al., 2012). The evaluation of the number and length of LSAs can be used as important factor in assessing the risk of recurrent ischemic stroke (Zhang et al., 2019).

In neurosurgical practice, the preservation of LSAs remains one of the most difficult tasks in insular glioma surgery (Pitskhelauri et al., 2021;

Table 1
Characteristics of preoperative and intraoperative data of 24 patients.

No of case	The number of LSAs		LSAs-tumor interface variant:		Histopathology, IDH1 mutation status	Cause of postoperative motor deficit
	3D-TOF MRA	Intraoperatively	3D-TOF MRA	Intraoperatively		
1	4	4	1	2	diffuse astrocytoma (IDH1+)	No new deficit
2	4	5	1	1	diffuse astrocytoma (IDH1+)	LSA injury
3	4	6	3	3	diffuse astrocytoma (IDH1-)	No new deficit
4	4	3	2	2	diffuse astrocytoma (IDH1+)	LSA injury
5	3	3	1	1	anaplastic astrocytoma (IDH1+)	LSA injury
6	6	6	2	2	diffuse astrocytoma (IDH1+)	No new deficit
7	2	2	2	2	oligodendroglioma (IDH1+)	No new deficit
8	0	3	3	3	diffuse astrocytoma (IDH1+)	No new deficit
9	3	3	1	1	diffuse astrocytoma (IDH1+)	No new deficit
10	4	4	2	2	diffuse astrocytoma (IDH1+)	LSA injury
11	6	5	3	3	anaplastic oligodendroglioma (IDH1+)	No new deficit
12	4	4	3	3	anaplastic astrocytoma (IDH1+)	No new deficit
13	4	4	1	1	diffuse astrocytoma (IDH1+)	No new deficit
14	7	5	1	2	anaplastic astrocytoma (IDH1+)	No new deficit
15	9	6	2	2	diffuse astrocytoma (IDH1+)	No new deficit
16	5	5	3	3	anaplastic astrocytoma (IDH1+)	LSA injury
17	4	4	3	3	diffuse astrocytoma (IDH1+)	No new deficit
18	4	4	3	3	diffuse astrocytoma (IDH1+)	No new deficit
19	6	6	1	1	diffuse astrocytoma (IDH1+)	direct damage of the IC
20	4	4	1	1	diffuse astrocytoma (IDH1+)	No new deficit
21	3	5	3	3	oligodendroglioma (IDH1+)	No new deficit
22	7	4	1	1	oigodendroglioma (IDH1+)	No new deficit
23	4	4	1	1	diffuse astrocytoma (IDH1+)	No new deficit
24	3	3	1	1	anaplastic oligodendroglioma(IDH1+)	LSA injury
	$\kappa = 0.508$ (95% CI: 0.2539; 0.7621) $\tau = 0.6447$ ($p = 0.0002$)		$\kappa = 0.873$ (95% CI: 0.7045; 1); $\tau = 0.9253$($p < 0.0001$) 1- LSAs encased by the tumor. 2- partial tumor growth around arteries. 3- LSAs pushed medially			The odds ratio (variant II or III vs variant I) - 3.18 (95% CI: 0.30–33.26).

Table 2
Clinical data of patients in related neurosurgical reports.

Author	Year	Number of patients	Type of study	Scanner	Modality Used	Assessment of the LSAs–tumor interface	Assessment of the number of LSAs	Intraoperative verification
Saito et al. (2009)	2009	3	Prospective	3T	3D TOF MRA with contrast	Yes	No	No
Bykanov et al. (2015)	2014	20	Prospective	3T	3D TOF MRA with contrast	Yes	No	No
Kawaguchi et al. (2014)	2014	83	Retrospective	3.0-T or 1.5-T	3D TOF MRA with contrast	Yes	No	No
Šteňo et al. (2016)	2016	2	Prospective	NA	3D TOF MRA	Yes	No	Yes (3DUS)
Rao et al. (2018)	2017	48	Prospective	1.5T	3D TOF MRA with contrast	Yes	No	No
Present study	2021	24	Prospective	3T	3D TOF MRA with contrast	Yes	Yes	Yes (IFA)

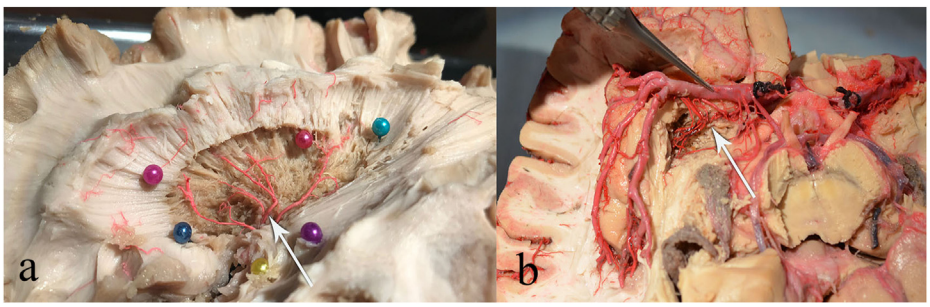

Fig. 3. Photographs of brain specimens. a: fiber dissection reveals vascularization of the basal ganglia and vascularization of the internal capsule by the LSAs (arrow). Colored needles show the boundaries of the insular lobe. **b:** anterior perforated substance and the LSAs (arrow).

Pitskhelauri and Bykanov, 2021). These arteries, as branches of the M1 segment of the middle cerebral artery, perforate the central and lateral parts of the anterior perforated substance (Fig. 3). Depending on where they branch from the M1 segment of the middle cerebral artery, they are divided into medial and lateral groups. Medial LSAs supply the head of the caudate nucleus, the central and medial portion of the putamen, the lateral segment of the globus pallidus, partly the anterior limb of the internal capsule and the anterior-superior part of the posterior limb (Marinković et al., 2001; Marinkovic et al., 1985). Lateral LSAs supply the upper part of the head of the caudate nucleus and the anterior limb of the internal capsule, most of the putamen, part of the lateral segment of the globus pallidus, and the upper part of the genu and the posterior limb of the internal capsule with the adjacent part of the corona radiata (Marinković et al., 2001; Tanriover et al., 2003).

Preoperative determining the course of LSAs and their relation to the tumor is an important factor influencing the selection of patients for microsurgical removal of the tumor. Given the practical importance of the problem of visualization of LSAs in the surgery of intrinsic insular tumors, many methods of their preoperative identification have been proposed: stereotactic cerebral angiography, CT angiography (Duffau et al., 2000), and the detection of arterial, T2 flow voids on MRI (Lang et al., 2001). However, due to the small diameter of LSAs, their visualization with non-invasive methods is not trivial (Šteňo et al., 2016). The most widely used non-invasive method of LSA visualization in clinical practice is 3D-TOF MRA at 1.5–3 T (Bykanov et al., 2015; Rao et al., 2018 ; Saito et al., 2009).

4.1. Intraoperative LSAs localization

The use of navigation systems to detect the LSAs intraoperatively is a difficult task. The LSAs usually are damaged during the final stages of tumor resection when significant brain shift has already occurred, causing target localization error. Reports on successful visualization of the LSAs by 3D ultrasound Doppler are available in the literature (Šteňo et al., 2016). Our experience is the opposite. It is difficult to detect the intraparenchymatous segment of the LSA 0.5–0.1 mm in diameter in the surgical wound during the final stages of tumor resection. The fluorescence videoangiography is a simple and reproducible method of real-time blood flow assessment allows visualization of small blood vessels. The use of fluorescence videoangiography helps to visualize the extraparenchymatous segment (and parent vessels) and confirm its integrity but provides no information about the course of the intraparenchymatous segment of the LSAs.

4.1.1. Assessment of the LSA–tumor interface

One of the limitations of 3D-TOF MRA in determining the relation between LSAs and glial tumor tissue is tumor tissue signal intensity in 3D-TOF MRA in cases of T1 isointense tumors (Bykanov et al., 2015; Rao et al., 2018). In these cases, it is impossible to determine the relation between the LSAs and tumor tissue. In a previously published paper (Bykanov et al., 2015), for such cases, additional 3D-T2 and 3D-T2-FLAIR sequences were recommended. This idea was later successfully implemented in the work of Rao et al. (2018). In the current article, we used the same approach, combining 3D-T2 and 3D-T2-FLAIR sequences with 3D-TOF MRA. As a result, the method demonstrated high sensitivity (100%, 95% CI: 0.63–1) and high specificity (86.67%, 95% CI: 0.58–0.98) in determining the LSA–tumor interface.

4.1.2. Assessment of the number of LSAs

In insular lobe glioma surgery, determining the relation of LSAs to a tumor is of primary practical importance. Relative to this task, determining the number of LSAs is associated with a lesser practical significance. Since there is often a wide dissection of the sylvian fissure and resection of the insula during surgery, it is possible to count the number of LSAs. This allowed us to compare intraoperative data with the results of 3D-TOF MRA for the first time and determine the sensitivity of 3D-TOF MRA in determining the number of arteries of such a small diameter. The number of LSAs according to the results of numerous anatomical studies varies widely from 1 to 21 (average = 5 to 10) (Bykanov et al., 2015; Marinković et al., 2001; Umansky et al., 1985; Türe et al., 2000 Türe et al., 2000; Marinkovic et al., 1985; Rosner et al., 1984). The average number of LSAs determined by 3D-TOF MRA according to the results of available imaging studies is smaller: 3.9 in Chen et al. (2011), 2.1 according in Kang et al., 4.1 in Chen et al. (Kang, 2009), 3 in Liang et al. (2019), 4.2 in Zhang et al. (2019), and 4.3 in our study. Understandably, doubts exist about the possibility of correctly identifying the number of LSAs using 3D-TOF MRA.

When 3D-TOF MRA findings were compared with intraoperative findings, we found that the average number of arteries determined by 3D-TOF MRA (4.3 ± 0.37) differed only slightly from the average value determined intraoperatively (4.25 ± 0.25), $\kappa = 0.51$ (95% CI: 0.25–0.76) and $\tau = 0.64$ ($p < 0.001$). An exact match between the numbers of arteries was observed in 15 (62.5%) cases. The discrepancy between the number of arteries determined by 3D-TOF MRA and intraoperatively is probably related to the insufficient resolution of 3.0 T MRI scanners. The use of 7.0 T MRI to visualize small-diameter perforating arteries could significantly improve the quality of the MR images obtained (Kang, 2009; Seo et al., 2012; Zhang et al., 2019; Harteveld et al., 2015; von Morze et al., 2007). However, 7.0 T MRI is not available in most clinical practices. Also, 3D-TOF MRA may be limited if the blood flow is perpendicular to the scanning plane as the TR is too short and protons do not have sufficient time for complete longitudinal relaxation, and it may be limited for small diameter LSA branches <0.3 mm that are below current voxel resolutions (Zhang et al., 2019). The LSAs could also be difficult to identify when a mass effect caused by tumor tissue causes a medial shift and an arcuate bend along the medial margin of the tumor.

The corticospinal tract can be supplied not only by the LSAs but also by the long perforating arteries that originate from the M2 segment of the middle cerebral artery. That is why identification and preservation of these arteries is one of the most important stages of surgical resection of the insula tumors. According to our anatomical study (Bykanov et al., 2015), long perforators from M2 in of 11% hemispheres reached the corona radiata. That is why in 2–3 patients in our series we could expect to detect these arteries using 3D-TOF MRA. However, in this series of patients they were not detected, presumably since they have a very small diameter, smaller than the LSAs.

5. Limitations

The higher resolution MRI scanner would have visualized LSAs of smaller diameter that may be undetected on the 3T MRI sequences. Due to strict inclusion criterias of the study, only 24 patients met the inclusion criterias and were included in the study.

6. Conclusions

The results of the current study demonstrated that in patients with insular gliomas, 3D-TOF MRA at 3.0 T is a highly sensitive method of characterizing LSAs. These results suggest that preoperative 3D-TOF MRA is a useful preoperative tool for neurosurgical planning and patient counseling.

Ethical approval

All procedures performed in studies involving human participants were in accordance with the ethical standards of the institutional and/or national research committee and with the 1964 Helsinki declaration and its later amendments or comparable ethical standards.

Informed consent

Informed consent was obtained from all individual participants

included in the study.

Availability of data and material (data transparency)

The datasets generated during and/or analyzed during the current study are available from the corresponding author on reasonable request.

Funding

This research did not receive any specific grant from funding agencies in the public, commercial, or not-for-profit sectors.

Conflict of interest

None.

Disclosure of funding

None.

Appendix A. Supplementary data

Supplementary data to this article can be found online at https://doi.org/10.1016/j.bas.2021.100856.

References

Bykanov, A.E., Pitskhelauri, D.I., Dobrovol'skiy, G.F., Shkarubo, M.A., 2015. Surgical anatomy of the insular cortex. Zhurnal voprosy neĭrokhirurgii imeni N. N. Burdenko 79 (4). https://doi.org/10.17116/neiro201579448-60.

Bykanov, A.E., et al., 2015. 3D-TOF MR-angiography with high spatial resolution for surgical planning in insular lobe gliomas. Zhurnal voprosy neĭrokhirurgii imeni N. N. Burdenko 79 (3). https://doi.org/10.17116/neiro20157935-14.

Chen, Y.C., Li, M.H., Li, Y.H., Qiao, R.H., 2011. Analysis of correlation between the number of lenticulostriate arteries and hypertension based on high-resolution MR angiography findings. Am. J. Neuroradiol. 32 (10). https://doi.org/10.3174/ajnr.A2667.

Chen, Y.C., Li, Y.H., Lu, J., bin Li, W., Wang, J.B., 2016. Correlation between the reduction in lenticulostriate arteries caused by hypertension and changes in brain metabolism detected with MRI. Am. J. Roentgenol. 206 (2). https://doi.org/10.2214/AJR.15.14514.

Duffau, H., Capelle, L., 2004. Preferential brain locations of low-grade gliomas. Cancer 100, 12. https://doi.org/10.1002/cncr.20297.

Duffau, H., Capelle, L., Lopes, M., Faillot, T., Sichez, J.P., Fohanno, D., 2000. The insular lobe: physiopathological and surgical considerations. Neurosurgery 47 (4). https://doi.org/10.1097/00006123-200010000-00001.

Eseonu, C.I., ReFaey, K., Garcia, O., Raghuraman, G., Quinones-Hinojosa, A., 2017. Volumetric analysis of extent of resection, survival, and surgical outcomes for insular gliomas. World Neurosurgery 103. https://doi.org/10.1016/j.wneu.2017.04.002.

Hameed, N.U.F., et al., 2019. Transcortical insular glioma resection: clinical outcome and predictors. J. Neurosurg. 131 (3). https://doi.org/10.3171/2018.4.JNS18424.

Harteveld, A.A., et al., 2015. High-resolution postcontrast time-of-flight MR angiography of intracranial perforators at 7.0 tesla. PLoS One 10 (3). https://doi.org/10.1371/journal.pone.0121051.

Hentschel, S.J., Lang, F.F., 2005. Surgical resection of intrinsic insular tumors. Neurosurgery 57 (1 Suppl. L). https://doi.org/10.1227/01.NEU.0000163603.70972.AB.

Hervey-Jumper, S.L., Berger, M.S., 2019. Insular glioma surgery: an evolution of thought and practice. J. Neurosurg. 130 (1). https://doi.org/10.3171/2018.10.JNS181519.

Kang, C.K., Park, C.A., Park, C.W., Lee, Y.B., Cho, Z.H., Kim, Y.B., 2010. Lenticulostriate arteries in chronic stroke patients visualised by 7 T magnetic resonance angiography. Int. J. Stroke 5 (5). https://doi.org/10.1111/j.1747-4949.2010.00464.x.

Kang, C.K., et al., 2009. Hypertension correlates with lenticulostriate arteries visualized by 7T magnetic resonance angiography. Hypertension 54 (5). https://doi.org/10.1161/HYPERTENSIONAHA.109.140350.

Kawaguchi, T., et al., 2014. Practical surgical indicators to identify candidates for radical resection of insulo-opercular gliomas. J. Neurosurg. 121 (5). https://doi.org/10.3171/2014.7.JNS13899.

Lang, F.F., et al., 2001. Surgical resection of intrinsic insular tumors: complication avoidance. J. Neurosurg. 95 (4). https://doi.org/10.3171/jns.2001.95.4.0638.

Liang, J., Liu, Y., Xu, X., Shi, C., Luo, L., 2019. Cerebral perforating artery disease: characteristics on high-resolution magnetic resonance imaging. Clin. Neuroradiol. 29 (3). https://doi.org/10.1007/s00062-018-0682-4.

Marinkovic, S.v., Kovacevic, M.S., Marinkovic, J.M., 1985. Perforating branches of the middle cerebral artery. Microsurgical anatomy of their extracerebral segments. J. Neurosurg. 63 (2). https://doi.org/10.3171/jns.1985.63.2.0266.

Marinković, S., Gibo, H., Milisavljević, M., Ćetković, M., 2001. Anatomic and clinical correlations of the lenticulostriate arteries. Clin. Anat. 14, 3. https://doi.org/10.1002/ca.1032.

Moshel, Y.A., Marcus, J.D.S., Parker, E.C., Kelly, P.J., 2008. Resection of insular gliomas: the importance of lenticulostriate artery position - clinical article. J. Neurosurg. 109 (5). https://doi.org/10.3171/JNS/2008/109/11/0825.

Pitskhelauri, D.I., Bykanov, A.E., 2021. Complication avoidance: resection of the insular glioma complicated by iatrogenic injury to the lenticulostriate artery. Acta Neurochir. https://doi.org/10.1007/s00701-021-04806-2.

Pitskhelauri, D., et al., 2021. Transsylvian insular glioma surgery: new classification system, clinical outcome in a consecutive series of 79 cases. Operative neurosurgery (Hagerstown, Md 20 (6). https://doi.org/10.1093/ons/opab051.

Rao, A.S., Thakar, S., Sai Kiran, N.A., Aryan, S., Mohan, D., Hegde, A.S., 2018. Analogous three-dimensional constructive interference in steady state sequences enhance the utility of three-dimensional time of flight magnetic resonance angiography in delineating lenticulostriate arteries in insular gliomas: evidence from a prospective clinicoradiologic analysis of 48 patients. World Neurosurgery 109. https://doi.org/10.1016/j.wneu.2017.09.199.

Rosner, S.S., Rhoton, A.L., Ono, M., Barry, M., 1984. Microsurgical anatomy of the anterior perforating arteries. J. Neurosurg. 61 (3). https://doi.org/10.3171/jns.1984.61.3.0468.

Saito, R., et al., 2009. Magnetic resonance imaging for preoperative identification of the lenticulostriate arteries in insular glioma surgery: technical note. J. Neurosurg. 111 (2). https://doi.org/10.3171/2008.11.JNS08858.

Seo, S.W., et al., 2012. Measurements of lenticulostriate arteries using 7T MRI: new imaging markers for subcortical vascular dementia. J. Neurol. Sci. 322 (1–2). https://doi.org/10.1016/j.jns.2012.05.032.

Šteňo, A., Jezberová, M., Hollý, V., Timárová, G., Šteňo, J., 2016. Visualization of lenticulostriate arteries during insular low-grade glioma surgeries by navigated 3D ultrasound power Doppler: technical note. J. Neurosurg. 125 (4). https://doi.org/10.3171/2015.10.JNS151907.

Tanriover, N., Kawashima, M., Rhoton, A.L., Ulm, A.J., Mericle, R.A., 2003. Microsurgical anatomy of the early branches of the middle cerebral artery: morphometric analysis and classification with angiographic correlation. J. Neurosurg. 98 (6). https://doi.org/10.3171/jns.2003.98.6.1277.

Türe, U., Yaşargil, M.G., Al-Mefty, O., Yaşargil, D.C.H., 2000. Arteries of the insula. J. Neurosurg. 92 (4). https://doi.org/10.3171/jns.2000.92.4.0676.

Umansky, F., et al., 1985. The perforating branches of the middle cerebral artery. A microanatomical study. J. Neurosurg. 62 (2). https://doi.org/10.3171/jns.1985.62.2.0261.

von Morze, C., et al., 2007. Intracranial time-of-flight MR angiography at 7T with comparison to 3T. J. Magn. Reson. Imag. 26 (4). https://doi.org/10.1002/jmri.21097.

Wang, Y., et al., 2017. Putamen involvement and survival outcomes in patients with insular low-grade gliomas. J. Neurosurg. 126 (6). https://doi.org/10.3171/2016.5.JNS1685.

Weller, M., et al., 2017. European Association for Neuro-Oncology (EANO) guideline on the diagnosis and treatment of adult astrocytic and oligodendroglial gliomas. Lancet Oncol. 18 (6). https://doi.org/10.1016/S1470-2045(17)30194-8.

Zhang, Z., et al., 2019. Visualization of the lenticulostriate arteries at 3T using black-blood T1-weighted intracranial vessel wall imaging: comparison with 7T TOF-MRA. Eur. Radiol. 29 (3). https://doi.org/10.1007/s00330-018-5701-y.